OFFICE OF NAVAL RESEARCH

Contract N00014-91-J-1641

R&T Code 313W001

TECHNICAL REPORT NO. 68

Electronic Characterization of Defect Sites on Si(001)-(2x1) by STM

by

V. A. Ukraintsev, Z. Dohnálek and J.T. Yates, Jr.

Submitted To

Surface Science

Surface Science Center
Department of Chemistry
University of Pittsburgh
Pittsburgh, PA 15260

February 27, 1996

Reproduction in whole or in part is permitted for any
purpose of the United States Government

This document had been approved for public release and sale;
its distribution is unlimited

19960313 089

DISCLAIMER NOTICE

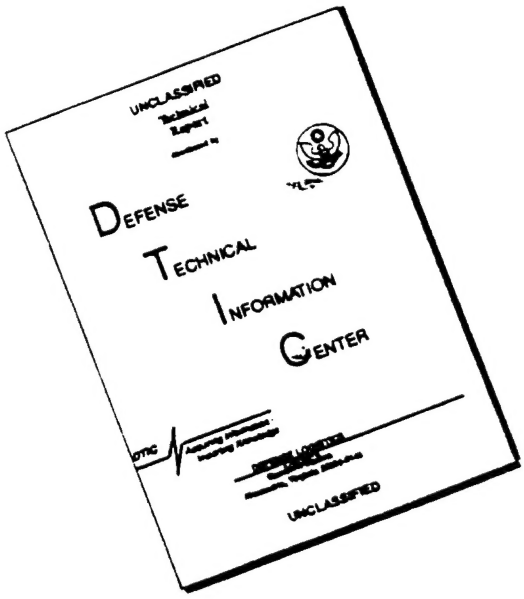

THIS DOCUMENT IS BEST QUALITY AVAILABLE. THE COPY FURNISHED TO DTIC CONTAINED A SIGNIFICANT NUMBER OF PAGES WHICH DO NOT REPRODUCE LEGIBLY.

REPORT DOCUMENTATION PAGE

Form Approved
OMB No. 0704-0188

Public reporting burden for this collection of information is estimated to average 1 hour per response, including the time for reviewing instructions, searching existing data sources, gathering and maintaining the data needed, and completing and reviewing the collection of information. Send comments regarding this burden estimate or any other aspect of this collection of information, including suggestions for reducing this burden, to Washington Headquarters Services, Directorate for Information Operations and Reports, 1215 Jefferson Davis Highway, Suite 1204, Arlington, VA 22202-4302, and to the Office of Management and Budget, Paperwork Reduction Project (0704-0188), Washington, DC 20503.

1. AGENCY USE ONLY (Leave blank)

2. REPORT DATE: February 27, 1996

3. REPORT TYPE AND DATES COVERED: Preprint

4. TITLE AND SUBTITLE
Electronic Characterization of Defect Sites on Si(001)-(2x1) by STM

5. FUNDING NUMBERS
N00014-91-J-1641

6. AUTHOR(S)
V.A. Ukraintsev, Z. Dohnalek and J.T. Yates, Jr.

7. PERFORMING ORGANIZATION NAME(S) AND ADDRESS(ES)
Surface Science Center
Department of Chemistry
University of Pittsburgh
Pittsburgh PA 15260

8. PERFORMING ORGANIZATION REPORT NUMBER

9. SPONSORING/MONITORING AGENCY NAME(S) AND ADDRESS(ES)
Office of Naval Research
Chemistry Division Code 313
800 North quincy Street
Arlington, Virginia 22217-5000

10. SPONSORING/MONITORING AGENCY REPORT NUMBER

11. SUPPLEMENTARY NOTES

12a. DISTRIBUTION/AVAILABILITY STATEMENT

12b. DISTRIBUTION CODE

13. ABSTRACT (Maximum 200 words)

A study of the defect sites on Si(001)-(2x1) was undertaken by employing Comparative Scanning Tunneling Spectroscopy (CSTS). Ni induced defects, the A, B, and C defects, and the A and B steps were studied. The STM tip induced band bending significantly affects tunneling spectra. This is evident from comparison of LDOS and local surface potentials obtained for high (10 Ω·cm) and low (100 Ω·cm) doped Si(001) crystals. Decay in the local surface potential was found around the Ni induced "split off dimer" defect site and in the "vacancy channel" defect. In agreement with previous studies, a reduction in the surface states energy gap was observed for the C defect. The B step and the C terrace defect reveal similar LDOS. This is interpreted as indicating that the C defect on the terraces migrates preferentially to the B step edge, and that it is due to a surface impurity such as Cl or a product of H_2O decomposition. This may be responsible for preferential etching phenomena or evaporation at step edges.

14. SUBJECT TERMS
silicon defects nickel STM

15. NUMBER OF PAGES

16. PRICE CODE

17. SECURITY CLASSIFICATION OF REPORT	18. SECURITY CLASSIFICATION OF THIS PAGE	19. SECURITY CLASSIFICATION OF ABSTRACT	20. LIMITATION OF ABSTRACT

Submitted to: Surface Science
February 27, 1996

Electronic Characterization of Defect Sites on Si(001)-(2×1) by STM

V. A. Ukraintsev, Z. Dohnálek and J. T. Yates, Jr.

University of Pittsburgh
Department of Chemistry
Surface Science Center
Pittsburgh, PA 15260, USA.

Electronic Characterization of Defect Sites on Si(001)-(2×1) by STM

V. A. Ukraintsev, Z. Dohnálek and J. T. Yates, Jr.

University of Pittsburgh
Department of Chemistry
Surface Science Center
Pittsburgh, PA 15260, USA.

A study of the defect sites on Si(001)-(2x1) was undertaken by employing Comparative Scanning Tunneling Spectroscopy (CSTS). Ni induced defects, the A, B, and C defects, and the A and B steps were studied. The STM tip induced band bending significantly affects tunneling spectra. This is evident from comparison of LDOS and local surface potentials obtained for high (10 Ω·cm) and low (100 Ω·cm) doped Si(001) crystals. Decay in the local surface potential was found around the Ni induced "split off dimer" defect site and in the "vacancy channel" defect. In agreement with previous studies, a reduction in the surface states energy gap was observed for the C defect. The B step and the C terrace defect reveal similar LDOS. This is interpreted as indicating that the C defect on the terraces migrates preferentially to the B step edge, and that it is due to a surface impurity such as Cl or a product of H_2O decomposition. This may be responsible for preferential etching phenomena or evaporation at step edges.

1. Introduction

Despite of technological importance of the Si(001) surface not much is known about an electronic structure of its defects. Hamers and Köhler[1] studied atomic-sized defects on Si(001). Using the Scanning Tunneling Microscope (STM), tunneling spectra *i.e.*, current vs bias voltage dependencies, were obtained for the A, B and C defects as well as for the regular Si(001)-(2×1) surface. However, no attempt was made to deconvolute the local density of states (LDOS) of the defects. Griffith *et al.*[2] examined the step geometry of Si(001)-(2×1) by STM but no electron spectroscopy has been accomplished. An energy of electronic states and a charge distribution on Si(001) steps have been calculated by Yamaguchi and Fujima.[3] Unfortunately, the difference between the calculated spectra and experimental data is very high.[4]

In this paper we report on local electron spectroscopy of defect sites of Si(001)-(2×1) obtained by a new tunneling spectroscopy technique, Comparative Scanning Tunneling Spectroscopy, CSTS.[5] This data evaluation technique reduces the influence of the tip condition on the sample LDOS deconvolution. We also employ the CSTS to monitor variations of local surface potential induced by defects.

2. Experimental

An ultrahigh vacuum (UHV) chamber with a background pressure of 2×10^{-11} Torr was employed for the experiments. The chamber was equipped with a STM (Omicron), a cylindrical mirror analyzer Auger spectrometer (Model 15-110, Physical Electronics Industries Inc.), and a quadrupole mass-spectrometer (100C, UTI).

Si(001) crystals (floating zone grown, p-type, B-doped, 10 and 100 Ω·cm, Virginia Semiconductor) with dimensions of $15\times4\times0.3$ mm^3 were cut from the silicon wafers by a diamond scriber, mounted on an etched-in-HCl Ta frame, ultrasonicated in pure ethanol, rinsed in deionized water and introduced into the UHV chamber through the load-lock system. After overnight outgassing at ~ 900 K, native oxide was removed from the Si(001) by a short (~ 60 sec) annealing at ~ 1450 K followed by slow (~ 2 K/sec) cooling. During annealing the background gas pressure was always below 1×10^{-9} Torr. STM images revealed a well organized (2×1) structure with traces of Ni contamination.[6]

The tips were prepared by the electrochemical etching of polycrystalline tungsten wire. Before use, the tips were annealed in UHV by direct contact with a tungsten filament preheated to ~ 2000 K. The tip condition was monitored by the STM imaging stability and by the Si(001)-(2x1) surface appearance.

Negative sample bias potentials of 1.3-1.4 V and tunneling currents of 0.25-0.375 nA were used as a reference for the feedback control during spectroscopy. To avoid silicon surface damage and to attenuate tip induced band bending[7], the tunneling current was always kept below 1 nA. In order to improve the signal to noise ratio, the data

acquisition time was at least 300 μsec long for the tunneling current measurement at each tip-sample bias voltage. Every presented spectrum is averaged over more than 100 individual current vs voltage curves obtained at similar defects.

The comparative LDOS of each type of defect is calculated by the following three step procedure justified elsewhere[5]:

(1) The differential conductivity vs bias voltage dependence was fitted by the asymmetric tunneling probability function:

$$F(S,V) = A_T T\left(S, {}^{eV}/_{2}\right) + A_S T\left(S, -{}^{eV}/_{2}\right), \qquad (1)$$

where $T(S,\xi) = \exp\left[-2S\sqrt{\frac{2m}{\hbar^2}(\overline{\Phi}-\xi)}\right]$ is the tunneling transmission probability; A_T and A_S are the proportionality coefficients related to the tip-surface effective contact area and these quantities are proportional to the tip and the sample densities of states at the Fermi level, respectively; S is the tip-sample separation; m and e are the electron mass and charge, respectively; $\overline{\Phi} = \frac{(\Phi_t + \Phi_s)}{2}$ is the average of sample Φ_s and tip Φ_t work functions; ξ is the tunneling electron energy referenced to the average of the tip and sample Fermi potentials; $\hbar$ is Planck's constant divided by 2π. $\overline{\Phi}$, A_T and A_S are the fitting parameters. S is assumed to be equal to 6 Å (see Section 4).

(2) The differential conductivity was normalized to the asymmetric tunneling probability function obtained from step (1). An individual LDOS is deconvoluted at this step.

(3) The difference between the individual LDOS determined for a defect site and a regular (2×1) site (the comparative LDOS) was calculated. This step was undertaken in order to reduce the tip condition influence on the deconvoluted LDOS difference.

This procedure provides highly reproducible comparative spectra of various defects and minimizes the influence of the spectroscopy parameters and the tip changes.

3. Results

3.1 Electronic Characterization of Defect Sites

An STM image of a defective Si(001)-(2×1) surface is shown in Figure 1. The image was obtained in a constant tunneling current mode at a positive sample bias potential of 1.0 V and a reference current of 0.5 nA. The majority of visible dimer vacancies are Ni induced, the "split off dimer" defects.[6] In the left top corner of the image, clusters of these "split off dimer" or Ni induced "vacancy channel" defects are seen.

Two terraces of Si(001) are shown. The A, B, and C defects[1] can be found on the terraces. Densities of the A and C defects show a general correlation with the transient background pressure during the crystal annealing and depend on the UHV chamber condition. We believe that these defects are induced by background gas adsorption during the crystal cooling following its annealing.

The B defect most frequently observed is a part of the "split off dimer" defect. Their density is correlated with the Ni surface concentration.[6]

The A and B step regions[8] can be seen along the edge of the top terrace (Fig. 1). The B step is always seen with the characteristic bright protrusions on the very edge.

Figure 2(a) presents the tunneling spectra, current vs bias voltage dependencies, obtained for the 10 Ω·cm, p-type, B-doped, Si(001) crystal. Curves for three different surface sites are shown: the regular (2×1) dimer, the Ni induced or the "split off dimer" defect,[6] and the C defect.[1] Corresponding deconvoluted individual LDOS plots are presented in Figure 2(b). These data for the non-defective (2×1) dimer sites are in reasonable agreement with the known LDOS of the ordered Si(001)-(2×1) surface.[4,9,10] Comparative LDOS for the Ni induced defect and the C defect are shown in Figure 2(c). The spectrum of the regular (2×1) dimer was used as a reference LDOS.

In Figure 3(a) tunneling current vs sample bias voltage dependencies for the 100 Ω·cm, p-type, B-doped, Si(001) crystal are presented. Curves for three different surface sites are shown: the regular (2×1) dimer, and the A step and the B step. Corresponding deconvoluted individual LDOS are presented in Figure 3(b). Comparative LDOS for the A and B steps, the Ni induced defect and the C defect are shown in Figure 3(c). In each case, the spectrum of the regular (2×1) dimer was used

as a reference LDOS. The spectrum of the Ni induced "vacancy channel" defect is similar to the "split off dimer" LDOS and, hence, is not shown. The A defect spectrum shows minor deviations from the regular (2×1) dimer LDOS and is also not shown.

The best fit parameters obtained during differential conductivity fitting by the tunneling probability function, eqn. (1), are presented in Tables 1 and 2 for the "high" and the "low" doped Si(001), respectively. If all four fitting parameters are used (A_T, A_S, S and $\overline{\Phi}$) then tip-sample separation S and work function $\overline{\Phi}$ are unreasonably high, $S \sim$ (13-25) Å and $\overline{\Phi} \sim$ (9-15) eV, respectively. For the feedback parameters employed one would expect an S value of ~ (5-6) Å and its minor variation (less than 1 Å) from one surface site to another.[11] Therefore, in order to diminish the observed discrepancy and to constrain the fitting procedure we assume $S = 6$ Å.

3.2 Spatial Characterization of C Defect

The cross-section of the C defect in two orthogonal directions, parallel and perpendicular to the dimer rows of the (2x1) structure, are presented in Figures 4(a) and 4(b), respectively. The STM image was obtained with a positive bias potential of 1.0 V applied to the sample and the reference feedback current of 0.5 nA. Depression with a characteristic lateral range from the C defect of 15-20 Å is seen in the direction parallel to the dimer row, Fig. 4(a).

4. Discussion

4.1 Tunneling Spectra Fitting Parameters for 10 Ω·cm and 100 Ω·cm Si(001)

Tables 1 and 2 present parameters which correspond to the best fit of the differential conductivity vs bias voltage dependence by the asymmetric tunneling probability function, eqn. (1). Band bending induced by the STM tip should affect the tunneling current vs bias voltage dependencies, especially, in the case of low doped silicon. [7] This phenomenon is not included in equation (1). Consequently, the fitting parameters (Tables 1 and 2) and, to a smaller degree, the deconvoluted LDOS (Figs. 2 and 3) should be affected by this factor.

The local surface potential or "local work function" obtained for the "high" doped Si(001) (Table 1) is comparable with values reported by Hamers and Köhler (cf. 2.5-3.0 eV, ref. 1). Conversely, the "local work functions" obtained for the "low" doped Si(001) crystal (Table 2) are too low. Most likely, this discrepancy is due to the strong tip induced band bending effect observed for the 100 Ω·cm Si(001) crystal, cf. the energy gap size in Figs. 2(b) and 3(b). Therefore, the tunneling probability fitting function, eqn. (1), should be improved. The band bending effect has to be considered for a low doped semiconductor. Therefore, in the following discussion we will focus on changes in the local surface potential obtained for the "high" doped, 10 Ω·cm, Si(001) crystal (Table 1).

4.2 The LDOS Variations and π States

Concerning the comparative spectra of the Si(001) defect sites (Figs. 2 and 3), one may emphasize that changes in LDOS occur at energies close to π electronic states of the dimerized surface Si atoms. These states are: the unoccupied π^* state at ~ (0.5-1.0) eV above the Fermi level, and the occupied π state at ~ (0.5-1.5) eV below the Fermi level.[4,12] Therefore, the density of these states (closest to the Fermi level) is sensitive to the bonding geometry of surface Si atoms and to their reactions with adsorbates.

4.3 Ni Induced and "Vacancy Channel" Defects

The LDOS of the Ni induced "split off dimer" and the "vacancy channel" defects (not shown) are similar. This is in agreement with their common origin.[6,13] Despite the significant rearrangements of surface Si atoms induced by the underlying Ni impurity,[6,13] the LDOS experiences almost no changes with respect to the normal (2×1) surface. Nevertheless, the local surface potential seems to be reduced in the vicinity of the "split off dimer" and "vacancy channel" defects (Table 1). This reduction in the local surface potential is also seen in the STM images as a slight elevation of the (2×1) surface around the Ni induced defects and, especially, in the "vacancy channel" vicinity (Fig. 1). As was shown by Koke and Mönch,[14] breaking of an asymmetric dimer with a large dipole moment may account for a significant local potential reduction of ~ 0.79 eV.

4.4 The C Defect and The B Steps of Si(001)

Spectra of the C defect, Figs. 2(c) and 3(c), show a pronounced peak at ~ 0.75 eV above the Fermi level and a modulation of the density of occupied states around ~ 1.0 eV below the Fermi level. Despite much discussion in the literature,[1,10,15,16] the origin of the C defect on Si(001)-(2×1) is still unclear. It was shown that atomic hydrogen,[10] water[15] and chlorine[16] adsorption may cause the appearance of the C defect. Unfortunately, we are not able to clarify the question since all above mentioned gases are present in the background gas of our UHV chamber during the crystal annealing and cooling.

In agreement with Hamers and Köhler,[1] we found a reduction in the energy gap size of the C defect spectrum, Fig. 2(a). Surprisingly neither the height elevation in the STM images (Fig. 1) or a decay in the local surface potential (Table 1) were observed around the C defect (cf. ref. 1). Just the opposite was observed; the (2x1) dimers are slightly depressed in the C defect vicinity as seen in a cross-section parallel to the dimer row, Fig. 4(a). No depression was observed in the cross-section perpendicular to the dimer row, Fig. 4(b); also no change in local surface potential was calculated (Table 1). The difference in the (2x1) surface appearance in two orthogonal directions argues against the local potential change or the local defect charging but rather suggests that the observed depression (or elevation ref. 1) in the

STM images due to the variations in LDOS at specific biases in the vicinity of the C defect.

Another possible reason for the discrepancy with the data of Hamers and Köhler may be the different doping of the Si(001) crystals used in these two studies.

An apparent difference between the C defect LDOS obtained in this paper and the one observed by Boland[10] for the H induced "bright ball-like" sites, probably, rules out the hydrogen adsorption as an origin of the C defect in our case. However, it should be mentioned here that an attempt to reproduce Boland's tunneling spectra acquisition conditions (feedback bias potential of +0.8 V, feedback current of 0.15 nA, bias ramp range of ± 2.5 V) led us to the very high, ~ 30 nA, tunneling current at the highest and the lowest biases. At such high tunneling current, damage of the Si(001) surface was regularly observed and the corresponding spectra were severely affected by silicon atom movement.

Interesting features were observed for the B step LDOS (Fig. 3). Overall the B step and the C defect spectra are quite similar. The B step LDOS reveals a reduction in the energy gap size and two peaks at ~ 0.75 eV above and below the Fermi level, Fig. 3(c). As was mentioned before, the characteristic bright protrusions which are visible on the very edge of the top terrace (Fig. 1) were always observed during the STM imaging of Si(001)-(2×1), and are unrelated to the density of the C defects on terraces. Two explanations for the similarity of the B step and the C defect LDOS

may be advanced: (1) The C defects are mobile during sample cooling and preferentially localize at the B step; (2) The B step and the C defect have similar bond geometry and electronic structure. We favor explanation (1) which suggests the role of an impurity adsorbate.

The selective location of the defects on the B step edge is a sign of special chemical properties of these sites and may explain preferential evaporation and chemical etching of the B step.

5. Conclusion

A study of local electron spectra of the defect sites on the Si(001)-(2x1) surface was undertaken by employing Comparative Scanning Tunneling Spectroscopy (CSTS). Ni induced defects, the A, B, C defects, and the A and B steps were studied (Figs. 2 and 3).

The tip induced band bending significantly affects tunneling spectra, especially, in the case of low doped silicon. This is evident from LDOS studied (Figs. 2 and 3) and from comparison of the local surface potential (Tables 1 and 2) for the "high" and "low" doped Si(001) crystals. Therefore, the tunneling probability fitting function, eqn. (1), should be improved. The band bending effect has to be considered in the case of low doped semiconductors.

A reduction of local surface potential was found around the Ni induced "split off dimer" and the "vacancy channel" defects (Fig. 1 and Table 1). The breaking of the asymmetric dimer, which has a significant dipole moment, may cause this local potential reduction.

In agreement with Hamers and Köhler,[1] we found a reduction in the surface states energy gap at the C defect, Fig. 2(a). At the same time, neither elevation in the STM images (Fig. 1) nor a decay in the local surface potential (Table 1) were observed around the C defect (cf. ref. 1). The observed anisotropy of the (2x1) surface depression around the C defect, Figs. 4(a) and 4(b), suggests that the effect is caused not by the local potential change or the defect charging but rather by LDOS variation around the C defect.

The characteristic bright protrusions observed on the B step edge (Fig. 1) reveal a spectrum similar to the C defect LDOS, Fig. 3(c). Taking into account this similarity we assume a common origin of these two defects. The selective location of the defects on the B step edge is a sign of special chemical properties of these steps and may explain their preferential evaporation and chemical etching.

Acknowledgment

The authors gratefully acknowledge the support of the Office of Naval Research.

Figure Captions

Figure 1. 400×400 Å STM image of Si(001). The image was obtained with a positive bias potential of 1.0 V applied to the sample. The raw data without any correction are presented. The various defects are indicated by arrows.

Figure 2. Site specific electron spectroscopy of Si(001) crystal (p-type, B-doped, 10 Ω·cm). The spectra were obtained with a negative reference bias potential of -1.3 V applied to the sample and a reference tunneling current of 0.25 nA. (a) Tunneling current vs sample bias potential dependencies. (b) Deconvoluted LDOS. (c) Deconvoluted comparative spectra. The LDOS of the normal (2×1) dimer was used as a reference.

Figure 3. Site specific electron spectroscopy of Si(001) crystal (p-type, B-doped, 100 Ω·cm). The spectra were obtained with a negative reference bias potential of -1.4 V applied to the sample and a reference tunneling current of 0.375 nA. (a) Tunneling current vs sample bias potential dependencies. (b) Deconvoluted LDOS. (c) Deconvoluted comparative spectra. The LDOS of the normal (2×1) dimer was used as a reference.

Figure 4. Cross-section of the C defect on Si(001)-(2x1): (a) parallel to the dimer row of the (2x1) structure; (b) perpendicular to the dimer row of the (2x1) structure. Sample bias potential +1.0 V, reference current 0.5 nA.

Table 1. The best fit parameters obtained during the differential conductivity fitting by the tunneling probability function, eqn. (1). The "high" (10 Ω·cm) doped Si(001). The tip - sample distance, S, was fixed to 6Å.

Parameters	$(2\times\bar{1})$ Dimer	"Split off Dimer"	C Defect
A_T	531	133	2819
A_S	1173	86	2237
S (Å)	6	6	6
$\overline{\Phi}$ (eV)	2.3	1.4	2.5

Table 2. The best fit parameters obtained during the differential conductivity fitting by the tunneling probability function, eqn. (1). The "low" (100 Ω·cm) doped Si(001). The tip - sample distance, S, was fixed to 6Å.

Parameters	(2×1) Dimer	"Split off Dimer"	C Defect	A Step	B Step
A_T	6.8	21.4	25.3	10.6	17.6
A_S	29.3	35.1	47.9	36.3	33.5
s (Å)	6	6	6	6	6
$\overline{\Phi}$ (eV)	0.95	0.99	1.01	0.97	1.02

References

[1] R. J. Hamers and U. K. Köhler, J. Vac. Sci. Technol. A7 (1989) 2854.

[2] J. E. Griffith, J. A. Kubby, P. E. Wierenga, R. S. Becker, and J. S. Vickers, J. Vac. Sci. Technol. A6 (1988) 493; J. E. Griffith, G. P. Kochanski, J. A. Kubby, and P. E. Wierenga, J. Vac. Sci. Technol. A7 (1989) 1914.

[3] T. Yamaguchi and N. Fujima, Surf. Sci. 242 (1991) 233.

[4] F. J. Himpsel and Th. Fauster, J. Vac. Sci. Technol. A2 (1984) 815

[5] V. A. Ukraintsev, Phys. Rev. B (1996) in press.

[6] V. A. Ukraintsev and J. T. Yates, Jr., Surf. Sci. (1996) in press.

[7] M. McEllistrem, G. Haase, D. Chen, and R. J. Hamers, Phys. Rev. Lett. 70 (1993) 2471; D. G. Cahill and R. J. Hamers, J. Vac. Sci. Technol. B9 (1991) 564.

[8] D. J. Chadi, Phys. Rev. Lett. 59 (1987) 1691.

[9] R. J. Hamers, Ph. Avouris, and F. Bozso, Phys. Rev. Lett. 59 (1987) 2071.

[10] J. J. Boland, Phys. Rev. Lett. 67 (1991) 1539; J. Vac. Sci. Tech. A10 (1991) 2458.

[11] C. Julian Chen, *Introduction to Scanning Tunneling Microscopy* (Oxford University Press, N.Y., 1993), p.6.

[12] J. Pollmann, P. Krüger, and A. Mazur, J. Vac. Sci. Technol. B5 (1987) 945.

[13] H. Niehus, U. K. Köhler, M. Copel and J. E. Demuth, J. Microscopy, 152 (1988) 735.

[14] P. Koke and W. Mönch, Solid State Communications 36 (1980) 1007.

[15] M. Chander *et al.*, Phys. Rev. B. 48 (1993) 2493.

[16] J. J. Boland, Science 262 (1993) 1703.

Figure 1
Ukraintsev, et al.

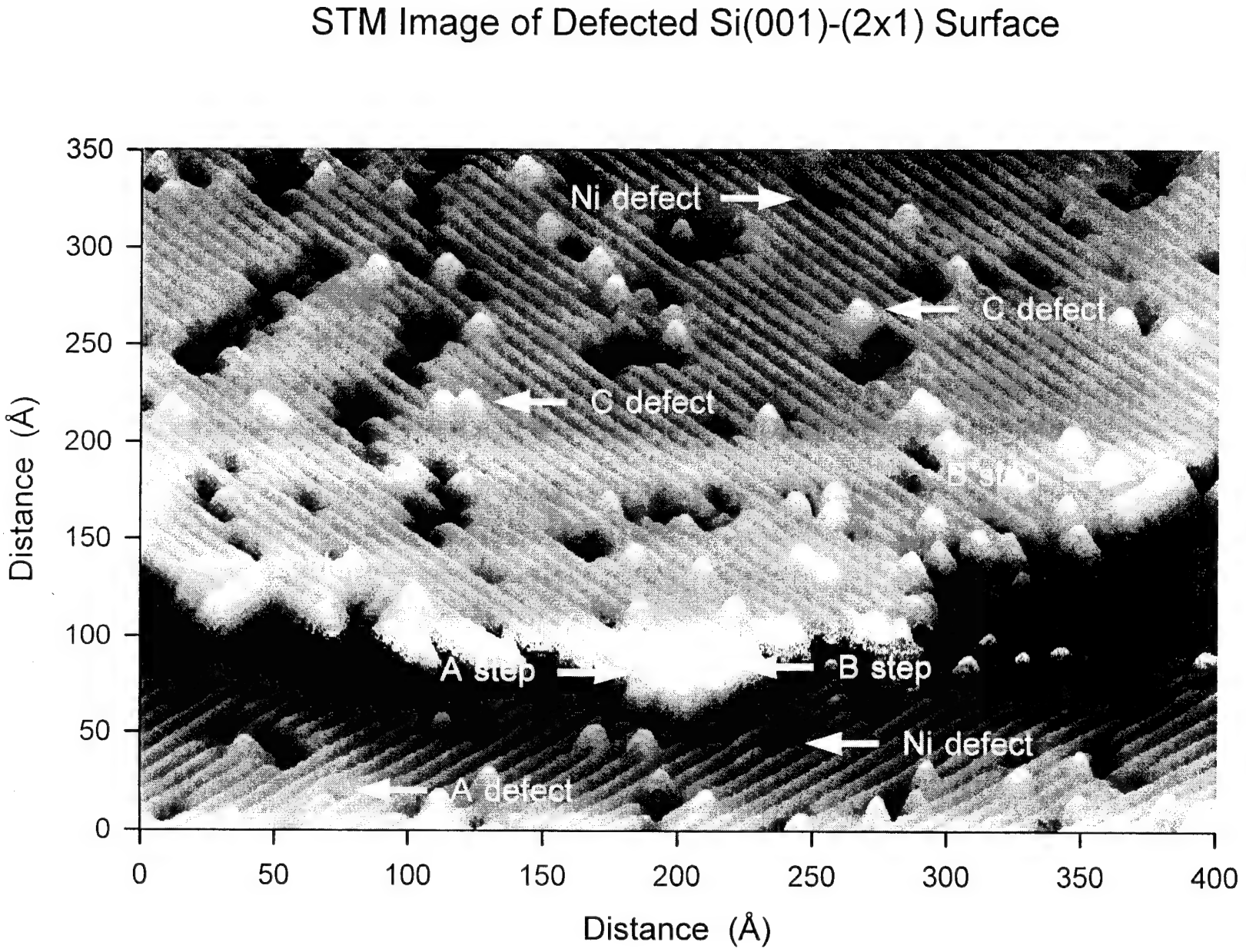

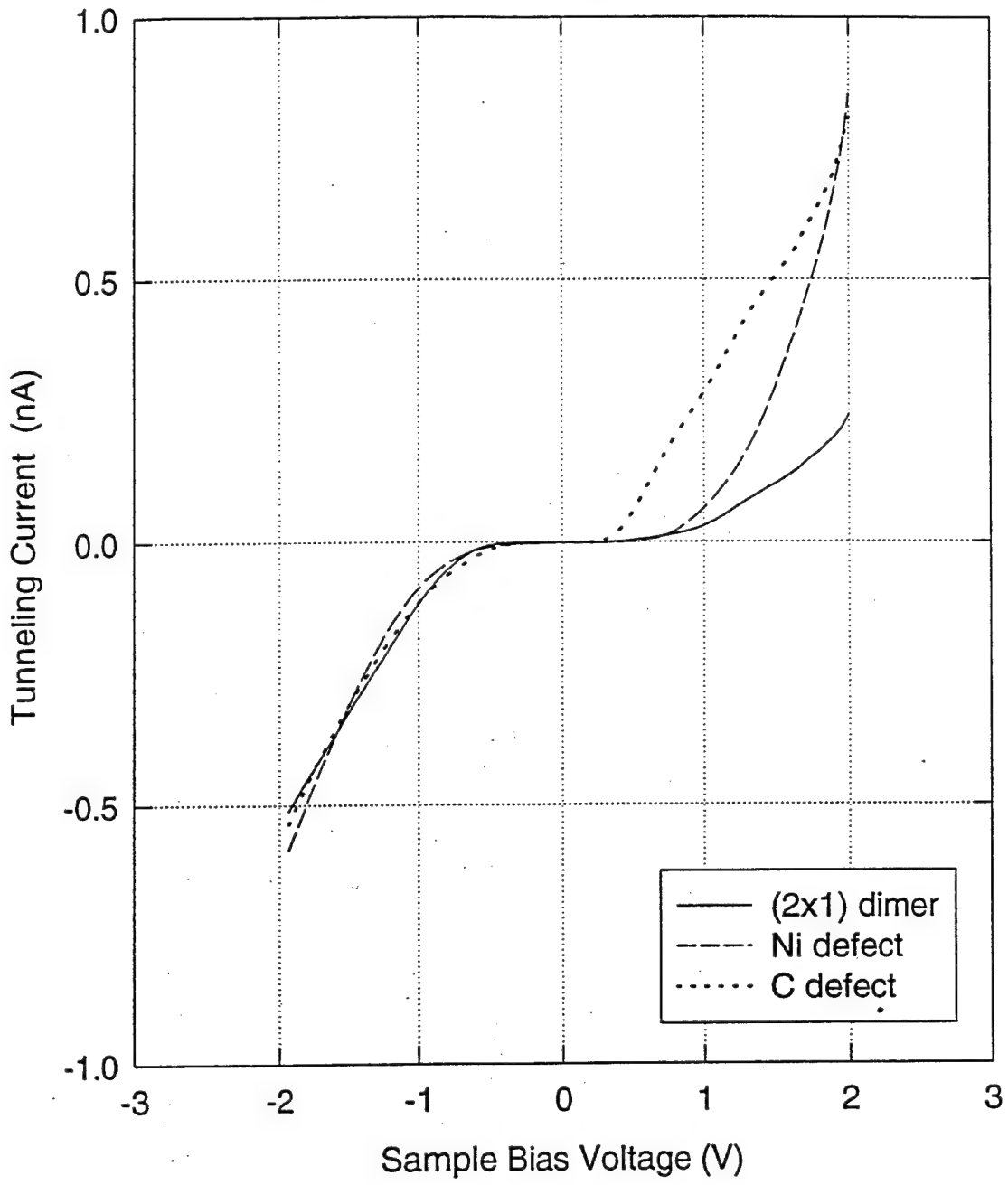

Figure 2(a)
Ukraintsev *et al.*

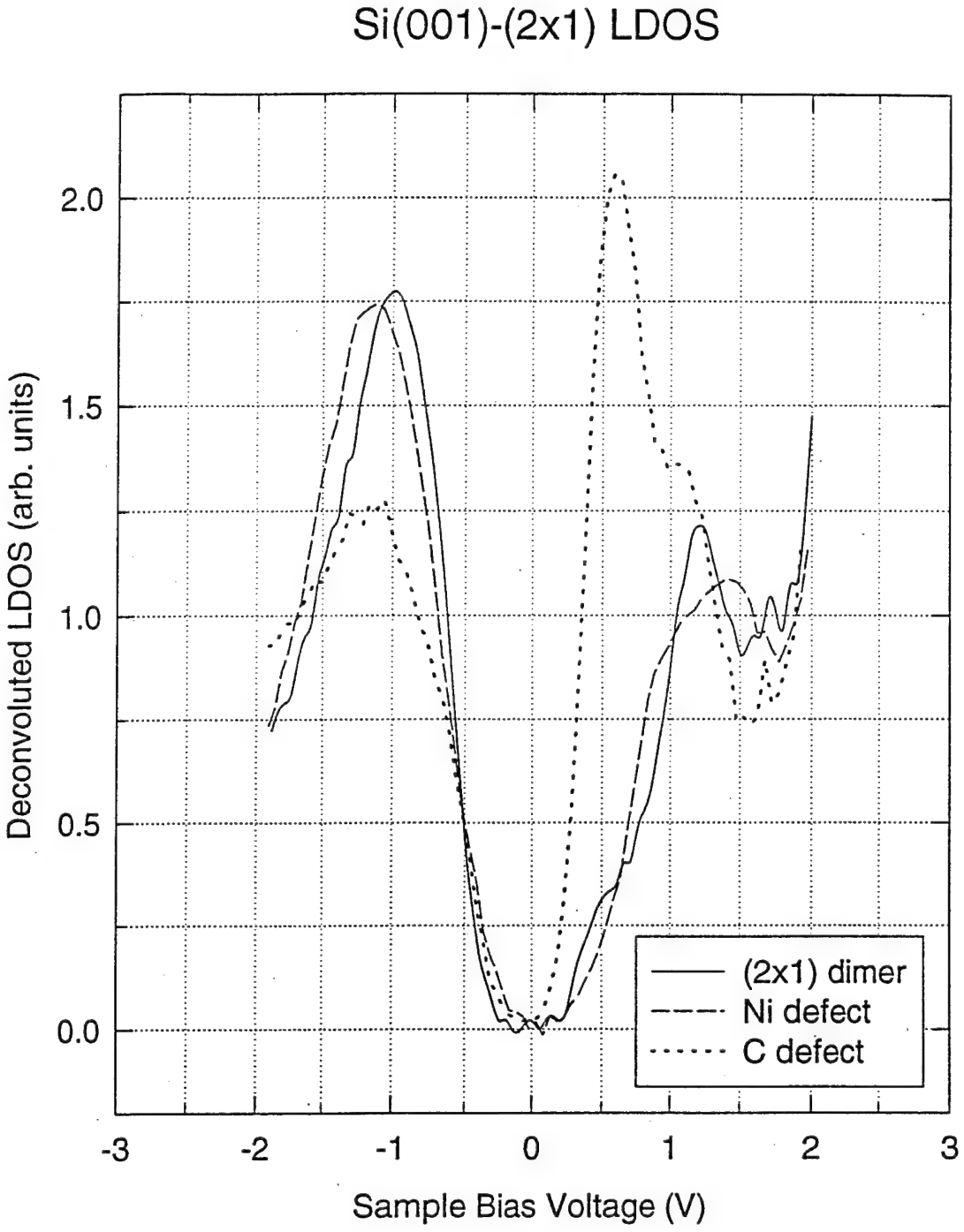

Figure 2(b)
Ukraintsev *et al.*

Site Specific Electron Spectroscopy of Si(100)-(2x1)

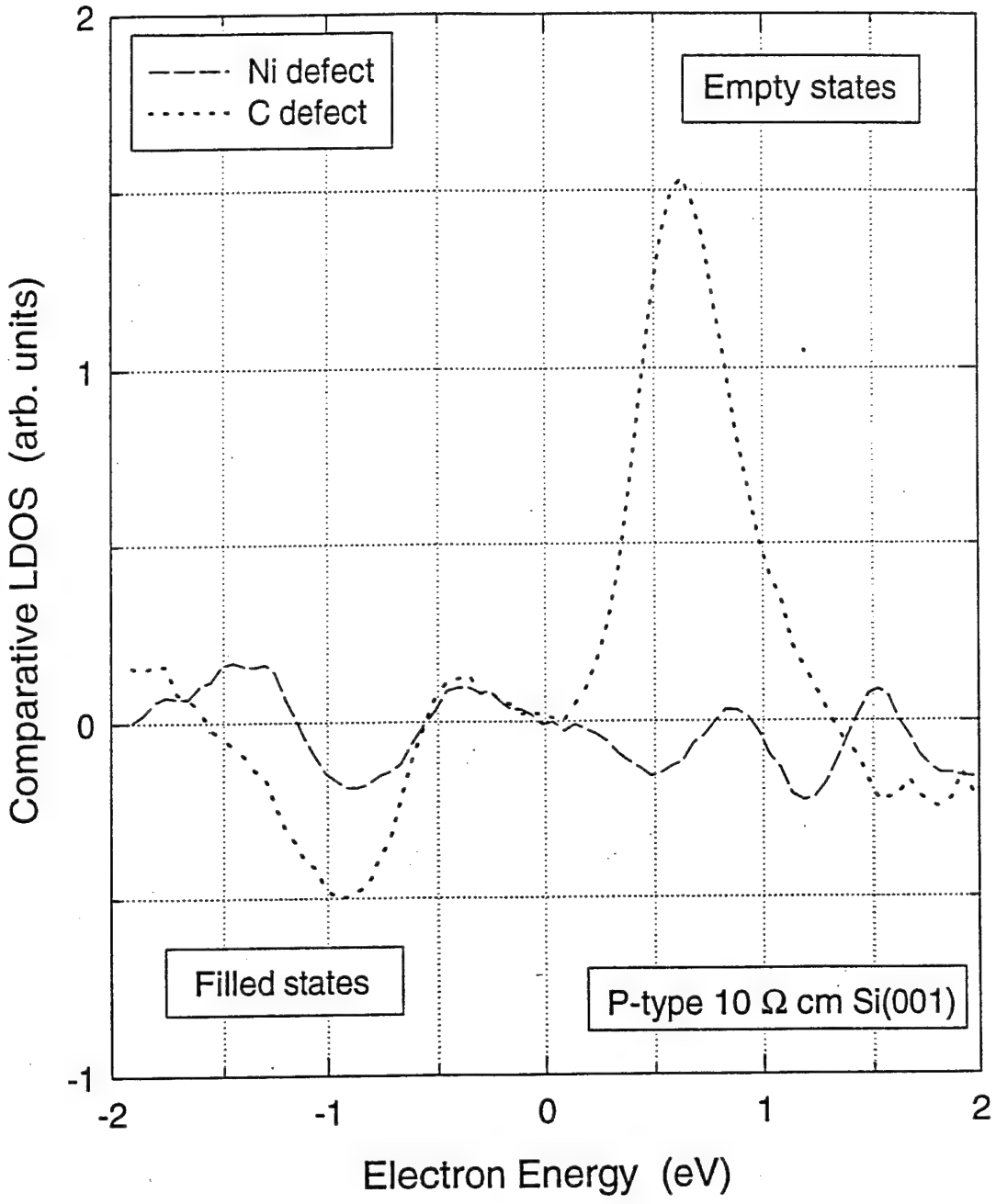

Figure 2(c)
Ukraintsev *et al.*

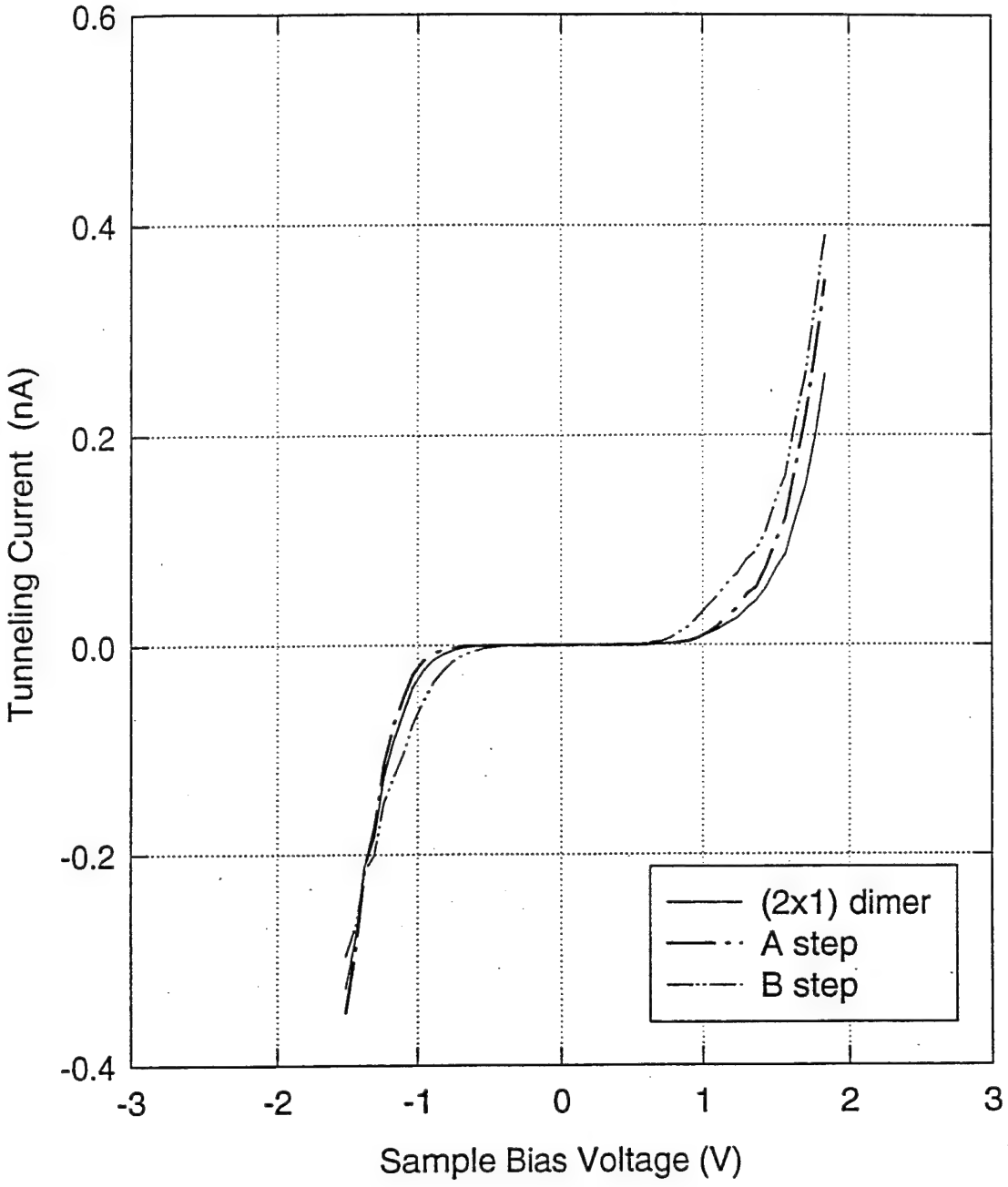

Figure 3(a)
Ukraintsev *et al.*

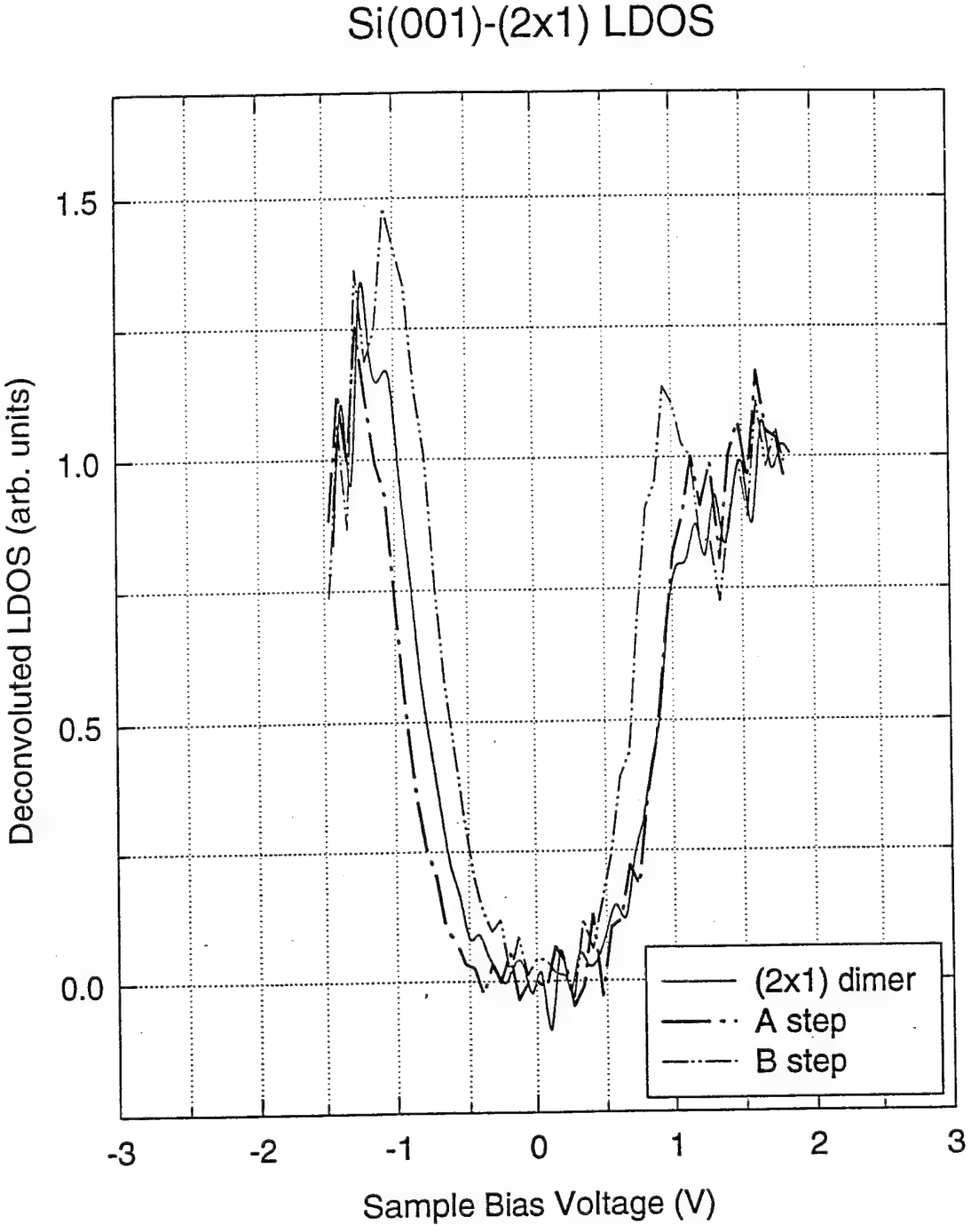

Figure 3(b)
Ukraintsev *et al.*

Site Specific Electron Spectroscopy of Si(100)-(2x1)

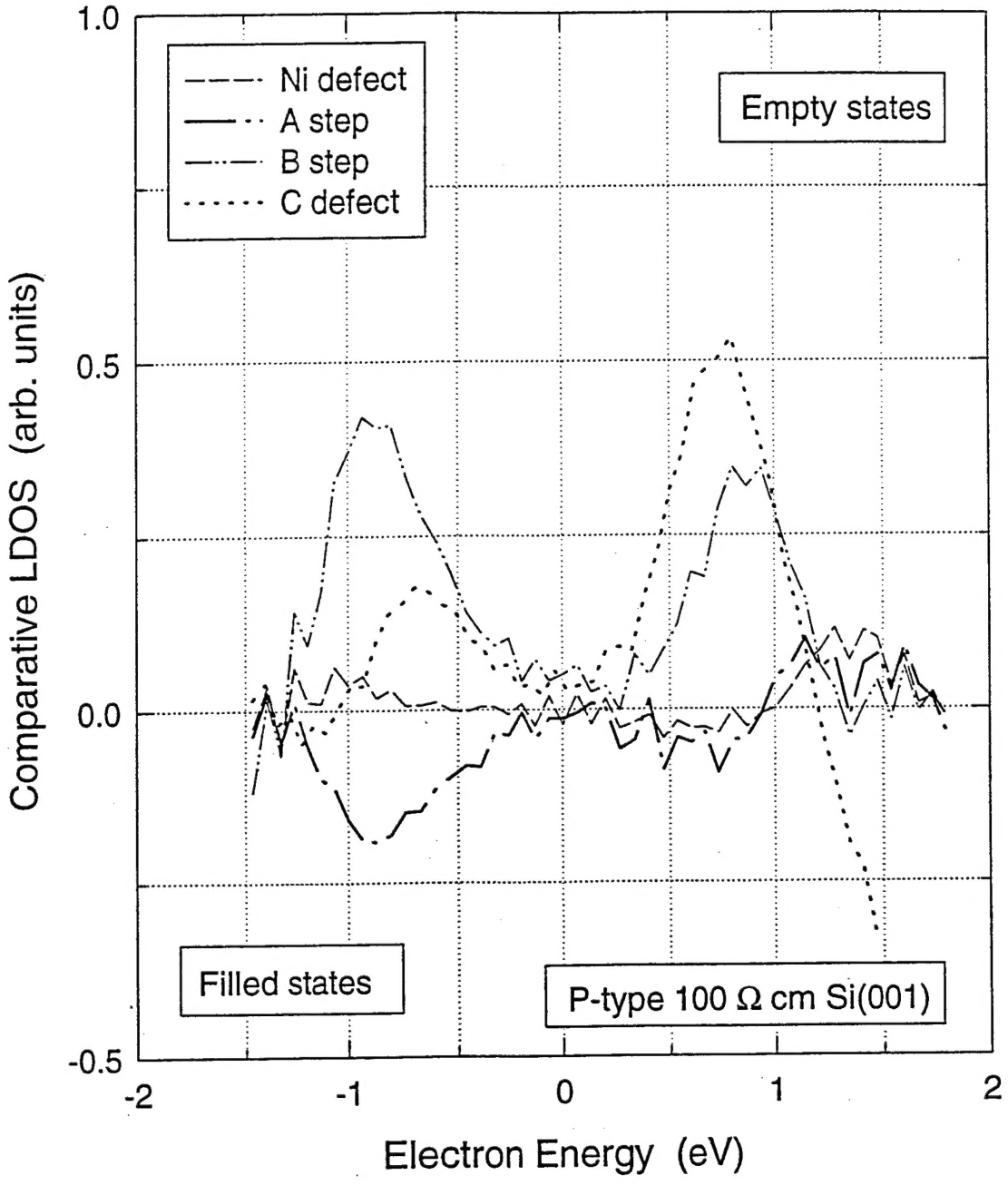

Figure 3(c)
Ukraintsev *et al.*

Cross-Section of C Defect in Direction Parallel to Dimer Row

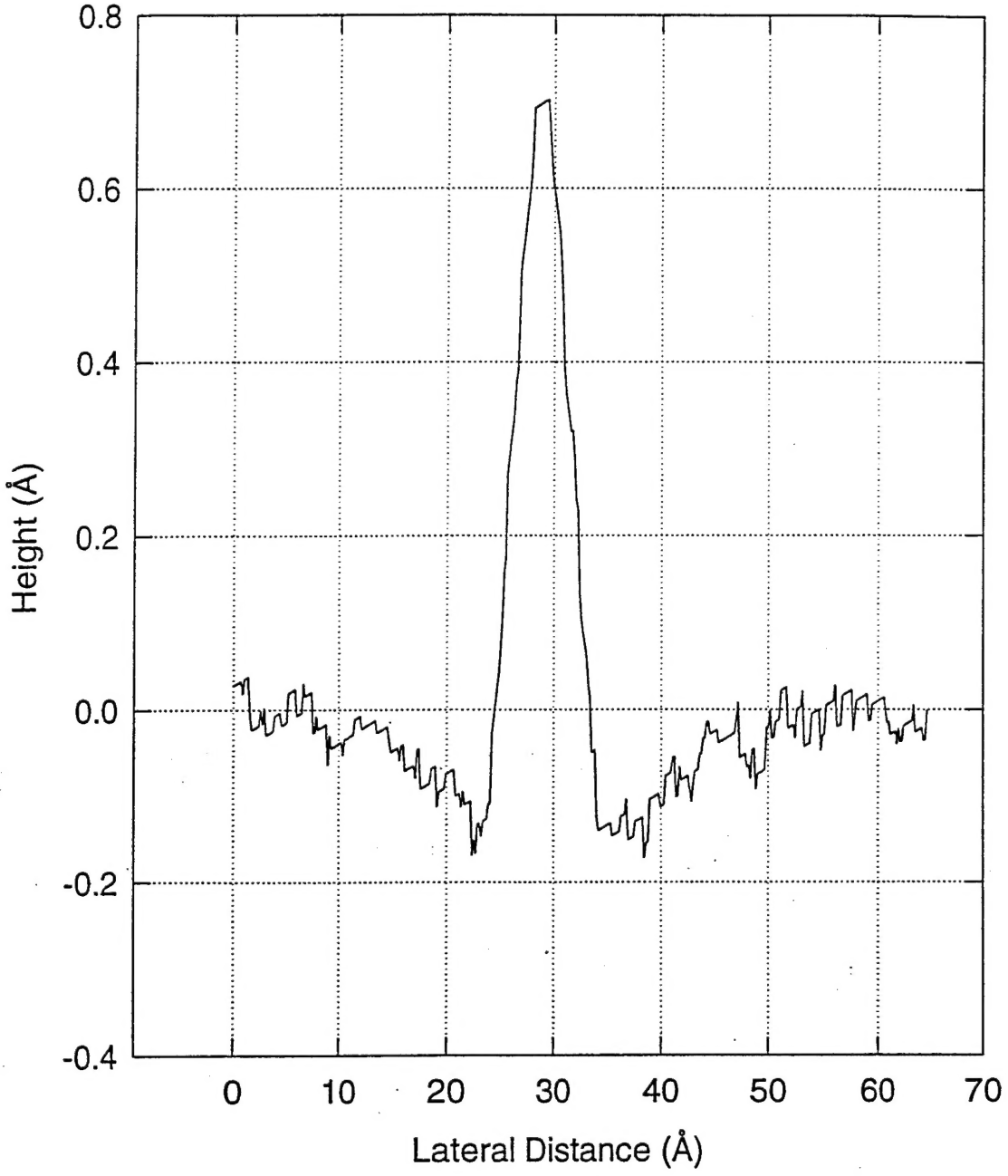

Figure 4(a)
Ukraintsev *et al.*

Cross-Section of C Defect in Direction Perpendicular to Dimer Row

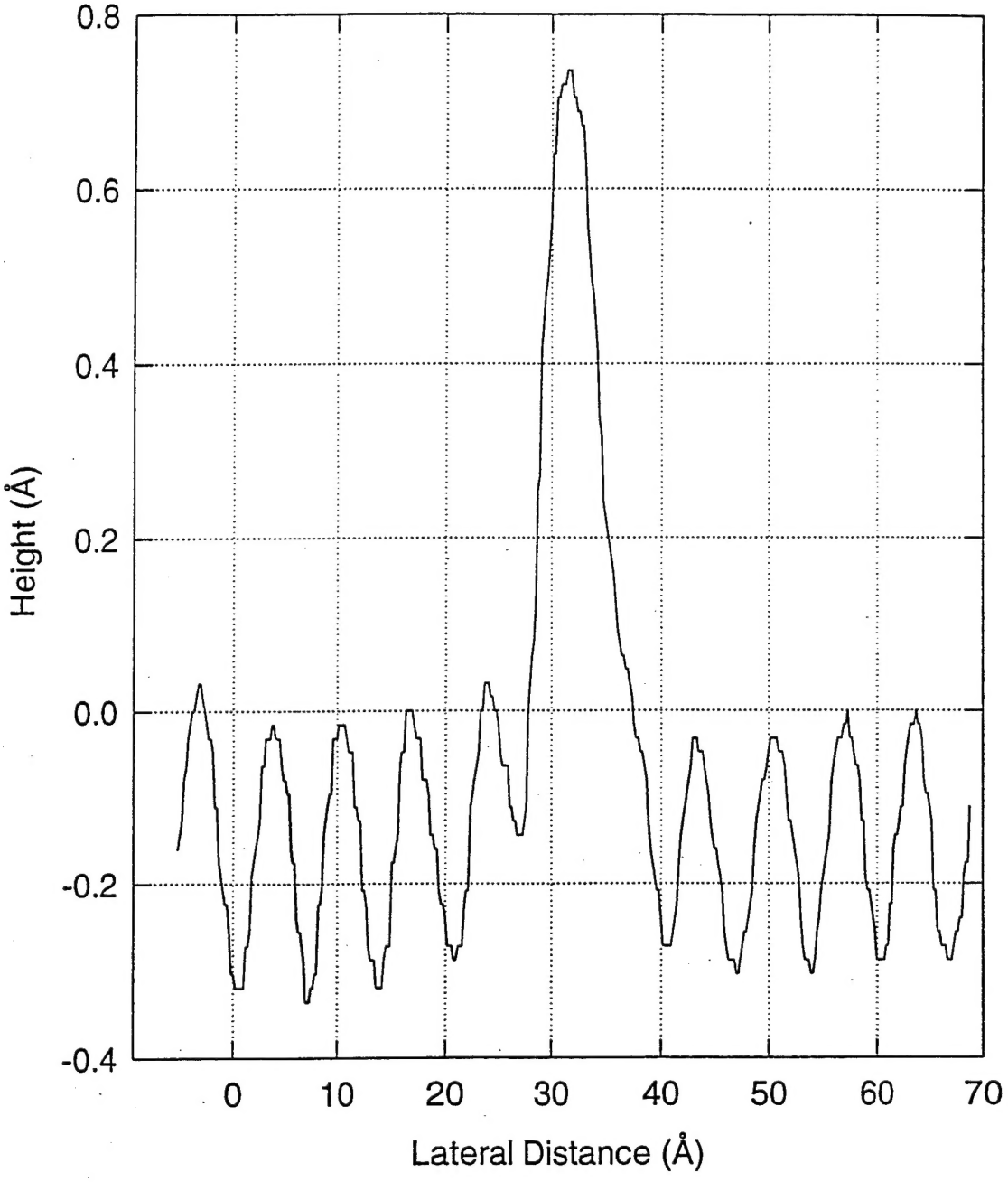

Figure 4(b)
Ukraintsev *et al.*

Dr. John C. Pazik (1)*
Physical S&T Division - ONR 331
Office of Naval Research
800 N. Quincy St.
Arlington, VA 22217-5660

Defense Technical Information Ctr (2)
Building 5, Cameron Station
Alexandria, VA 22314

Dr. James S. Murday (1)
Chemistry Division, NRL 6100
Naval Research Laboratory
Washington, DC 20375-5660

Dr. John Fischer (1)
Chemistry Division, Code 385
NAWCWD - China Lake
China Lake, CA 93555-6001

Dr. Peter Seligman (1)
NCCOSC - NRAD
San Diego, CA 92152-5000

Dr. Bernard E. Douda (1)
Crane Division
NAWC
Crane, Indiana 47522-5000

* Number of copies required